Simulation of Water in a Small Pore: Effect of Electric Field and Density

Michael E. Green* and Jianjun Lu

Department of Chemistry, The City College of the City University of New York, 138 Street and Convent Avenue, New York, New York 10031

Received: April 9, 1997; In Final Form: May 28, 1997[⊗]

The behavior of water in a pore of nanometer dimensions is studied by Monte Carlo simulation over a series of densities, and with five different electric charge configurations, providing external fields from zero to extremely high values, exceeding 3×10^9 V m^{-1}. The pore contained a tapered section that had an opening of radius 0.25 nm into a secondary tapered section below. The pore wall was a medium of dielectric constant 4 (comparable to the value in a protein), and the electric charges were placed in the wall. A reservoir, with which the remainder of the volume could exchange water molecules, was kept at constant density. Quantities that were obtained included the energy of the system, the orientation of the water molecules in the tapered section of the pore (and the remainder of the volume, but that proved to show little orientation), the density in response to the density of the reservoir section, molecular distributions, and electric potential and field. We observed that a high field, as expected, lowered the energy of the water molecules, the density of the pore responded to the density of the reservoir, and the orientation of the molecules in the tapered section responded to the field of the fixed charges in the wall. The larger fields pulled molecules close to the wall, on average. The differences in the behavior of the tapered section and the cylindrical section are particularly interesting: small changes in geometry produce significant changes in water structure and apparent rigidity as shown by the high average orientation. To the extent that the pore can be thought of as a model for a protein channel, it suggests that small changes in an amino acid side chain, whether by mutation, proton transfer, or simply reorientation, could have major consequences for the function of the protein; this includes geometric effects, as well as effects upon the electric field, and through the field, on the water in the pore.

I. Introduction

Water in pores has been the subject of extensive studies, both experimental and theoretical. It exists in biological systems, especially proteins, which are of greatest interest here.[1−8] There is also a substantial literature in other fields, including mineralogical[9,10] and colloidal and interfacial systems.[11−13] Not only do such systems contain water in pores but the water plays a major role in the determining the properties of at least some of these systems. We have a particular interest in the gating of ion channels in membranes, and the calculations presented here are intended to help decide whether it is reasonable that the water is significant in these processes (plural, as gating varies somewhat among even similar channels). In earlier work, we have suggested that the water controls the gating;[14,35] we are here interested in whether density effects are involved and whether high electric field produces effects that may be compared to the effects of changes in density.

High electric fields have drastic effects on the water in pores. Coupling to density changes may be expected to be important; the increase in density of water in the high field found in the electrical double layer has been measured at a silver electrode by Toney et al.[15,16] A theoretical treatment of the electrostriction of water in these high fields by Danielewicz-Ferchmin and Ferchmin[17] has provided an apparently successful attempt to account for the near doubling of density, compared to bulk water, found by Toney et al.

A substantial literature is devoted to extending the Poisson−Boltzmann equation at flat interfaces, with a number of methods proposed, including the modified Poisson−Boltzmann equation of Outhwaite and Bhuiyan[18] and a somewhat different approach by Attard et al.[19]

The most common method of studying the interface has been simulation. A number of workers have considered the effects of boundaries, and others the effects of electric fields. High-field simulations at interfaces, particularly the electrical double layer,[20−22] have shown the expected orientation effect in the high field and the increase in density. What is more, these three studies suggested the existence of a phase transition by the water at sufficiently high field. Simulations at high field are important in double-layer systems as well as proteins, which are known to have high fields present. A Stark effect measurement by Lockhart and Kim[23] of the field near the end of peptide gave a field of 0.43×10^9 V m^{-1}; the end of a peptide is a fairly low field region by comparison with a surface of pore with charges. Theoretical work by Lancaster et al.[24] gave fields much higher than the end-of-peptide value (by approximately an order of magnitude) in the *Rhodopseudomonas viridis* reaction center. Finally, our own calculation also leads to similar order of magnitude fields.[25]

In addition to the determination of the density of water in the high field found in the double layer by Toney et al,[15,16] Wiggins and co-workers[26] have reported both increased and decreased densities of water in gel networks, the sign of the effect depending on hydrophobicity. Thanki et al.[27] gave experimental evidence for the existence of ordered water adjacent to charged residues in a number of proteins.

Simulations have produced similar results. It has been shown that fields above approximately 10^9 V m^{-1} produce orientation and increased density of the water in the double layer. Watanabe, Reinhardt, and Brodsky[21,22] studied the behavior of water in the high fields of the electric double layer and found increased ordering and density, as well as the apparent phase transition mentioned above. Sansom and co-workers[28] found ordering and wall effects in model pores similar to those

* e-mail: green@scisun.sci.ccny.cuny.edu.

[⊗] Abstract published in *Advance ACS Abstracts,* July 15, 1997.

S1089-5647(97)01220-0 CCC: $14.00

considered here. In addition, Sankararamakrishnan et al.[29] have considered the effects of solvation on a model of a protein channel, the pore domain of the nicotinic receptor, and although the particular model is not critical, the general behavior of the water is relevant.

There have been a number of simulations of a particular channel, gramicidin, in which the water lines up single file, with semi-microscopic studies by Jordan, Partenskii, and co-workers being particularly instructive.[30,31] Single-file behavior makes results on this channel less relevant to our work, but they do illustrate the point that the behavior of water can strongly influence, or determine, how the channel acts in the presence of ions.

In earlier work we[14] have proposed that water, partially immobilized by charges on the protein, is responsible for the gating of channels. Different charge states of the protein can lead to different behavior of the water and thus to differing conductivity for ions. The behavior of the water under these conditions can couple to the electrostatic effects on ions.

Ion channels found in biological membranes have water-filled pores of dimensions such that 30−50 molecules are in the critical region of the pore. These channels are defined by protein walls which contain charges, and our previous results[25,35] lead to calculated fields in excess of 10^9 V m^{-1}. In this respect we agree with the results found by Lancaster et al.[24] on the *R. viridis* reaction center, not a channel protein in the same sense as we are considering the term, but with enough structural similarity to be relevant.

It may also be of interest to know how the channels behave under less natural conditions of increased pressure; experimental values of density vs pressure have been measured for several crystal forms of ice, up to pressures in excess of 100 GPa, greater than values relevant for our purposes.[32,33] Calculations in the direction of lower density may also provide insight into the development of possible trends as a function of density. A second reason for going to lower density is the lower activity of the water; in this sense, it resembles the effect of adding an impermeant solute to the bulk liquid outside the pore. The analogy with the results of osmotic pressure experiments is imperfect, as the means of lowering the free energy of the water is relevant, so we will not pursue the question in detail. However, it does suggest a means of approaching the simulation of osmotic pressure experiments.

For these reasons, we have carried out Monte Carlo simulations of water in a model pore. We chose dimensions approximately those of a biological channel; however, the results should apply to any system of the same approximate size and configuration. The channel is in equilibrium with a reservoir, held at constant number of molecules (*N*), volume (*V*), and temperature (*T*). With *NVT* held constant, it is not possible to also hold chemical potential constant. However, it is possible to calculate this quantity, although it will fluctuate. The remainder of the system must be in equilibrium with the reservoir, so that changing the number of molecules in the reservoir puts the remainder of the system in equilibrium with a system at differing density, and therefore differing pressure.

The pore wall can also be considered an abstract representation of the protein channel wall; water molecules may be permanently attached to avoid excessive hydrophobicity, and a dielectric constant assigned to replace the protein. Using the dielectric constant within the wall and explicit water in the pore, we can calculate the electric field associated with various distributions of charges and apply this field to the water. Therefore, the system can be studied as a function of charge distribution and pressure (or density). We have done so using a model for water that is polarizable, to allow for the effects of the high fields which we find from the fixed charges, plus the fields produced by the water molecules themselves. The importance of polarizability in water has been further demonstrated by Gregory et al.[36] Whether the PSPC model is the best possible or not, it is almost certainly better to include at least an approximate correction for polarizability than to omit it and use a point charge model.

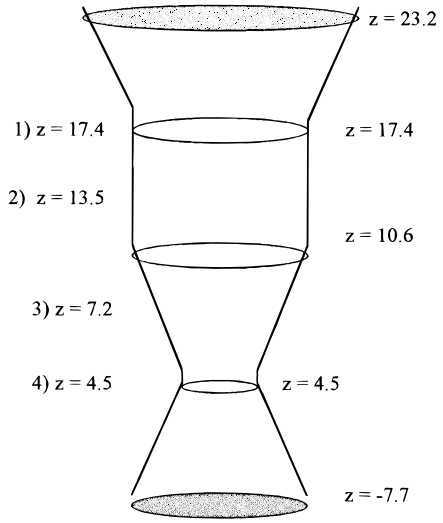

Figure 1. Model of pore. A projection of the model is shown. The labels show the dimensions of the pore. Charges are placed in four rings, at values of *z* equal to 4.5, 7.2, 13.5, 17.4; up to four charges can be placed in one ring at 90° angles. The upper unfilled ring and the central ring define the *cylinder*, and the central ring and the lower unfilled ring the *tapered section*. The zero of *z* is placed at the apex of the cone formed by the tapered section above the constriction, so that the bottom of the lowest section is at $z = -7.7$ Å. The radius at the constriction, which has a height of 1.0 Å (not indicated) is 2.3 Å, for the entire cylinder 5.5 Å, and at the top of the volume 8.5 Å. The dielectric constant in the simulation volume is determined by explicit water molecules; it is 4 in the walls and 80 above and below the simulation volume. There are a total of 28 water molecules attached to the walls, of which 12 are attached to the bottom, above the −7.7 Å level.

The simulations have been analyzed in terms of the energy of the water, the orientation of the water, the distribution of the molecules, and density of the water in the parts of the channel other than the reservoir. We have found the water to be partially oriented, with the orientation increasing at the highest charge. The behavior of the energy and the density of the remainder of the pore as a function of the change in density of the reservoir are also reported. The water behaves, in response to field and density, in a manner consistent with possible participation of water in ion channel gating.

II. Model and Methods

(1) Pore Model. The particular pore model we have studied is described in Figure 1. The model tapers to a narrow section, of diameter approximately appropriate for one ion to pass. The results reported here use a radius at the narrowest ring of radius 2.5 Å. Finally, the lowest section allows the water molecules to pass through the narrow section and assists with equilibration. However, properties of this lower section are not being studied in this work, and it is somewhat isolated from the remainder of the pore; it does help make the part of the system of primary interest more realistic. We will refer to the upper region as the *reservoir* and the region below the cylinder and above the constriction as the *tapered region*. The cylinder and the tapered region are the parts of the system of greatest interest.

Take the zero for the z axis to be at the apex of the cone formed by the tapered region, were it continued downward to complete the cone. Measured from this point, section boundaries z coordinates, in Å, are as follows: reservoir, upper boundary, 23.3; reservoir to cylinder, 17.5; cylinder to tapered region, 10.7; tapered region, lower end, 4.5; short section (constriction), lower end, 3.5; lower boundary, −7.7. The tangent of the angle formed by the nonvertical walls with the z axis is 0.5236, for an angle of 27.6°.

(2) Calculation. *(a) The Electric Field and Potential*. The technique is the same as that which we have described earlier.[14,25] We will therefore offer only a brief summary here. Charges are included in the dielectric medium (dielectric constant $\epsilon = 4$, as appropriate for a protein[34,23]). For a general charge position, whether within or outside the pore, the potential and field are calculated at all points on a 2 Å lattice. The technique places induced charges on the boundary and uses these with Coulomb's law to find the potential and field. The boundary is divided into sections 1 Å × 1 Å over most of the boundary, but 0.5 Å × 0.5 Å in the highest field region, and the surface charges are taken to be the average over this area. It is possible to solve for the induced charges at each segment from the contribution of the fixed charges, the induced charges on all other elements, and the contribution of the individual elements. The result is a set of linear simultaneous equations for the induced charges, to which the solution allows the determination of the potential and field elsewhere simply from Coulomb's law.

The 2 Å lattice distance for fields and potentials in the entire space (not the boundary) is as small as it can be while fitting within computer memory without delaying the simulation to an impractical extent. Given the cylindrical symmetry, it is only necessary to have two dimensions for the source points, in addition to the three dimensions for the field points; the source points can be placed along a line which is rotated to get the third dimension each time the field is required. The same arrays of field and potential are used for the water molecules in the pore (which include point charges in the polarizable model used) and the charges fixed in the dielectric medium. In use, the arrays are read into memory; the field components and potential appropriate for the actual positions of the source and field points are found by linear interpolation among the nearest lattice positions (four points for the two dimensions used for the source, eight for the three dimensions in field).

(b) Simulation. A Monte Carlo simulation was carried out on the water molecules, in the manner described in our earlier papers.[25,35] Briefly, the water in the pore was set up to have an icelike structure initially. In our previous work, 4000 Monte Carlo steps per molecule were allowed for equilibration, followed by 2000 steps per molecule for data collection. In those cases, we started with densities close to the final values, so that the 4000 step per molecule equilibration was adequate. Here, we are not necessarily near equilibrium density to start, so we performed the following test for equilibration: for each of three values of reservoir density, 61% of normal, 100% of normal, and 113% of normal, and with the five charge configurations used for all the computations reported here (see section iv), the initial number of molecules in the cylinder was set equal to 5, 10, and 20 in separate runs. Two runs for each charge and each initial density were carried out. It turned out that 4000 steps/molecule gave indistiguishable results, both for density and energy, for 5, 10, or 20 molecules placed initially in the cylindrical section. Since the normal starting density in the cylindrical section is 13 molecules, we accepted 4000 steps/molecule equilibrium as appropriate for these runs, for all values of the density of the reservoir. Two thousand steps/molecule were used for data collection after equilibration. The data shown are averages of three runs for each set of parameters, for a total of 180 runs (3 runs/set of 12 values of number of reservoir molecules, and 5 charge configurations). This entire procedure was repeated for the two configurations of water molecules fixed to the walls (with and without rotation permitted: see below). By doing three separate equilibrations followed by data collection we ensured that no peculiarity of any one run could have an excessive influence.

(c) Water Model. The water model used was the PSPC (polarizable simple point charge) model of Ahlstrom et al.[36] It places charges on the H (+0.3345 electron charges) and O (−0.6690 electron charges) atoms and allows for polarizability on the O atom. It has been used for our previous papers as well. The polarizability is included because the fields are high enough to cause the molecules to have significant induced dipoles (for details, see Ahlstrom et al.[36]). There is also a Lennard-Jones energy, centered on the oxygen atom. The polarizability requires self-consistency; we have approximate self-consistency by updating the field at each molecule each Monte Carlo step for that molecule, so that the field is never more than one step behind and always includes the most recent step of each other molecule when a molecule makes a step. We also added a 2.5 Å hard core around the oxygen to the PSPC model to avoid the "polarizability catastrophe" which can occur when neighboring molecules generate large attractive potentials when they come too close together (Ahlstrom et al. used an increased van der Waals repulsive energy to accomplish the same purpose). This value does not appear to have prevented the requisite increase in density. A cube 2.5 Å on a side is 15.6 $Å^3$ in volume, or approximately 52% of the normal volume per water molecule. Density did not increase above the bulk value by more than approximately 20%. If we went to extremely high compression, the model would become more problematical. The value at which we stopped should allow the water to still behave normally, without the average intermolecular distance decreasing so greatly as to distort the molecules significantly. However, we do not know that the PSPC model has been independently tested at high and low densities, and there may be additional error from this source. As we saw no gross indications of improbable behavior to the extent of our investigations, we are willing to accept the results as at least sufficiently quantitative for the conclusions we have drawn.

(d) Charge and Density as Independent Variables. (i) Charge. Five charge states were studied. One had no fixed charges; the others, four different configurations of charges. Charges were placed in four rings holding a maximum of four charges each, at 90° angles. The charge locations can be understood from Figure 1 and are 1.5 Å outside the boundary, at values of z of 4.5, 7.2, 13.5, and 17.4 Å, where $z = 0$ is defined as the apex of the cone formed by the tapered region; it is 7.7 Å above the bottom of the model, as shown in Figure 1. One configuration had no charge. The lowest nonzero charge configuration had charges of −1 at each of the two lower rings and of +2 at each of the two upper rings. Another configuration had charges of −2 at each of the two lower rings and +2 at each of the two upper rings. A higher charge configuration had charges of −3 at the lowest ring, −2 at the next lowest, +2 at the third ring, and +3 at the highest ring. In addition, another configuration had the same net charge as the middle configuration, but with three negative and one positive (i.e., (−3,+1)) charges to create the −2 charge on the two lower rings; this had the largest number of total charges, but two pairs

were arranged as dipoles, in effect. The zero-charge case is the fifth configuration.

(ii) Density. The reservoir shown as the upper section in Figure 1 (above $z = 17.5$ Å) was held at a constant number of molecules throughout any one simulation, by restoring the number after each sequence of 1 step/molecule. The number of molecules in this section was set at 20, 21, ..., up to 31 molecules. With 26 molecules in the reservoir corresponding to bulk density, we went from approximately 20% above bulk density to approximately 20% below. We designate the fixed reservoir number of molecules n_{res}.

(e) Initial Placement of Water Molecules. (i) Mobile Molecules. The molecules are initially placed on an ice lattice within the simulation volume, which is in turn shrunk 10% in volume, uniformly, to approximate the density of liquid water. The exception in this work is the density of the upper "reservoir", which is an independent variable, adjusted as described in section iv.b.

(ii) Nonmobile Molecules. Two classes of nonmobile molecules were also used in the simulation, to line the walls and make them less hydrophobic. (i) Bottom section: Two layers with a total of 12 molecules were placed in the bottom of the lowest section, to allow a buffer region in which the dielectric constant could adjust to the external value of 80 at that boundary. (ii) Others: Several rings of molecules, always paired, were placed in the upper section of the volume. These had their oxygen atoms either 0.5 or 1.1 Å from the walls, depending on which direction the dipoles were pointing. Two complete sets of runs were carried out, for two methods of placing the molecules on the wall: (1) The molecules were paired but allowed to rotate for 1000 steps at the beginning of the equilibration part of the run. The consequence for the potential was severe. The molecules found a minimum energy position that gave a net dipole, this in turn contributing a significant potential, comparable to that of more than one charge. After the first 1000 steps per molecule, these molecules were not allowed further motion, so there were a set of *fixed dipoles*. (2) The molecules are paired and not allowed to rotate, with the pairing arranged so that the dipole practically cancels, leaving at most a quadrupole field which is small compared to the previous dipole field or to the field produced by charge in the wall of the model. The results are rather different for this case than for the case of rotating wall molecules, as the fields are smaller. There are *no fixed dipoles* in this case. The wall was still made reasonably hydrophilic, as would be required for a model of a protein, for example. We will primarily report the results from this set, as the field introduced by the water dipoles does not necessarily correspond to a part of the physical model we wish to study. However, the results from both are instructive, especially for the zero-charge case, and we will refer to the dipolar results as appropriate.

In both cases, there are a total of 28 molecules that are not allowed to translate, eight below the constriction, four in the tapered section above the constriction, eight in the cylindrical section, and eight in the reservoir section. None of these molecules are counted in the density plots resulting from the simulations. All density data refer to the mobile molecules.

(f) Analysis of Results. (i) Graphs. All one-dimensional plots were done using the Plot program (version 1.2, Fortner, Inc.); curve fits and, for linear fits, least squares slopes and intercepts and correlation coefficients were calculated by the program. The program also calculated averages and standard deviations. For three-dimensional plots (potential plots), the Slicer program from the same package was used.

(ii) The molecular distributions were obtained by analysis of the positions of the molecules at the end of the simulations and are the result of averaging over three sets of positions, obtained in independent runs, for each distribution. With the wall molecules not rotating (no fixed dipoles), the positions of the molecules after 4000, 5000, and 6000 steps per molecule were used; with the fixed dipoles case, only results after 6000 steps per molecule were kept.

(iii) All other quantities were averaged over the 2000 step data collection phase of the simulation, with the results then averaged over the three runs for each density and charge configuration. All subsequent averaging is described in the section where it is reported below.

III. Results

We are primarily concerned with the following variables as functions of the density in the upper section of the pore: orientation of the water molecules with respect to the field and *z* axis (main axis) of the pore; density in the two sections below the upper section (reservoir), the cylinder, and the tapered region, energy of the water molecules, distribution of the molecules with respect to the walls, intermolecular distances, and electrical potential and field throughout the volume. Each of these has been determined for each of the charge states, as described in section II.d.i.

(1) Energy. *(a) Energy of Molecules in Reservoir (Upper Section, above $z = 17.3$ in Figure 1).* The upper section is distant from the charges and experiences a relatively small electrical potential and electric field as a result. For this reason, one expects the energy to be fairly close for all charge configurations, as indeed is found from the simulations within statistical error. In our earlier work,[35] in which the reservoir was held at approximately bulk density, 26 molecules, we determined the chemical potential of the molecules in the reservoir, as well as the average energy. In that study water dipoles were allowed, through the rotation of wall-attached molecules in the first 1000 steps per molecule. (Note that in that study the lower part of the present simulation volume was absent; the model was truncated at the narrowest section.) In that case, the chemical potential turned out to be equal to the value found by Ahlstrom *et al.*,[36] 38 kJ/mol. The average energy (not free energy) per molecule in the earlier work was -0.30×10^{-19} J; in this work it averages -0.27×10^{-19} J/mol when the number of molecules in the reservoir is 26, and the water dipoles are present. Considering the statistical error, we can regard this as quite close; there may also be a small contribution from the charges, which were different in the earlier work. This is a small system, so one must allow for somewhat larger statistical errors than in a system which is much larger. Standard deviations are given with the data, below; they are on the order of 10%. There may also be a small contribution from the charges, which were different in the earlier work; the -0.27×10^{-19} J value consists of an average over charges, for $n_{res} = 26$ (n_{res} is the number of molecules in the reservoir). However, with the water dipoles absent, the average $E_{res} = -0.34 \times 10^{-19}$ J/mol; this becomes 0.37×10^{-19} J/mol with the average intercept added. (One expects that if the dependence is perfectly linear, leading to no energy in the absence of molecules, the intercept should be zero. However, it is the latter value that should be compared to the -0.30×10^{-19} J/mol found earlier.) There is more than statistical error involved, as can be seen from a comparison of the reservoir energy *per molecule* for the water dipole and no water dipole cases.

With Fixed Water Dipoles. For all charge states, in units of 10^{-19} J, the average energy per molecule in the reservoir is

TABLE 1: Energy[a] of Mobile Water Molecules in the Tapered and Cylinder Sections

charge distribution	tapered section energy	±standard deviation	cylindrical section energy	±standard deviation
(0,0,0,0)	−0.202	0.016	−0.225	0.016
(−1,−1,2,2)	−0.268	0.026	−0.255	0.015
(−2,−2,2,2)	−0.305	0.027	−0.277	0.019
((−3,1),(−3,1),2,2)	−0.470	0.029	−0.293	0.029
(−3,−2,2,3)	−0.376	0.051	−0.303	0.020

[a] Units of $\times 10^{-19}$ J/molecule.

$$E_{av} = -0.0061(\pm 0.0010)n_{res} - 0.11(\pm 0.02) \qquad (1)$$

where the stated errors are one standard deviation, averaged over the five different charge configurations, which are taken to be effectively identical. In the reservoir, the charges produce a relatively small effect, as they are set far from the reservoir. As the number of molecules increases and the intermolecular interactions become stronger, the energy per molecule is affected. The effect is of moderate size; eq 1 shows that adding each molecule provides a nearly 6% increment to the average energy per molecule. This is presumably a consequence of the smaller intermolecular spacing as the density increases in a range in which the interactions are favorable.

We do not see an energy minimum at bulk density.

No Fixed Water Dipoles. The appearance of the energy is quite different. For this case,

$$E_{av} = -0.013n_{res}(\pm 0.001) - 0.03(\pm 0.03) \qquad (2)$$

The intercept in this case cannot be distinguished from zero, and the relation is again linear. The slope is double its previous value. Evidently there is a contribution to the energy from the water dipoles fixed to the wall, and this is in part compensated by some other term, which approximately balances it at normal density. We are not certain of the nature of the compensation at this time, but it is not surprising that the water molecules interact with dipoles which are free to orient differently from their interaction with water molecules held rigidly. It may be that the more favorable interactions suggested by the large negative intercept for the rotating water molecules do not exist when the molecules are fixed, but the molecules add more favorable interactions with each other to compensate. Testing this point remains for future work.

(b) The Other Water Molecules. No Fixed Water Dipoles. The energy of the water molecules that are not in the reservoir is significantly affected by the charges, on average. We will discuss primarily the case in which no water dipoles are fixed to the wall, separately for each charge configuration, for the cylinder and the tapered section. Again in units of 10^{-19} J, Table 1 gives the energy of the water molecules, in the two important sections, for each charge configuration. These averages are taken over all values of the number of molecules in the reservoir. The variation with density in the average energy per molecule is less than the standard deviation and is therefore ignored. We can see that increasing the charge lowers the energy. For the tapered region, the energy could be written approximately as

$$E_{tap} = -0.032N_1 - 0.20 \qquad (3)$$

where N_1 = number of charges in the lower two rings and units are 10^{-19} J. The lower two rings are those at the level of the tapered section. The net charge does not matter, as the (−3,1),(−3,1),(2,2) configuration fits the relation if counted as eight charges, not four. Apparently the interaction is fairly local. It is also clear that the cylinder has a much weaker interaction with the charges, as expected from the size of the cylinder; this is also reflected in the orientation data. The interaction is certainly not zero, and the interaction with the charges in the lower rings also has some effect, as the three middle configurations in Table 1 each have four charges in the upper rings, but do not have quite the same average energy for cylinder water molecules. However, it is obvious that these effects are weak compared with the effect in the tapered section. Since there should be approximately as many water molecules near the upper charges as the lower, the effect here is not entirely local; the larger volume dilutes the field, possibly by interactions with other waters which are polarized to reduce the field.

With Fixed Water Dipoles. The energy of the molecules in the *presence* of the water dipoles showed that for all molecules taken together a change of about 3×10^{-19} J, total, existed between the highest charged and zero-charge state. This amounts to about $75k_BT$, even though there is a large field from the water dipoles always present. This energy is large enough to determine the biological function of a channel. Qualitatively, one would come to a similar conclusion for the case of the dipoles as for the case of no dipoles.

(2) Orientation. Only part of the simulation volume is in a high enough field to produce significant orientation of the molecules. Danielewicz-Ferchmin and Ferchmin[17] found that above an average field of 2.64×10^9 V m^{-1} the orientation of water molecules is essentially complete in the field, with the average cosine of the water dipoles with respect to the field reaching unity. The orientation of the water molecules in this work is primarily of interest in the tapered region. Our results for this region are shown in Table 2. The walls are evidently responsible for some of the orientation and may not orient the molecules in the same direction as the field.

The average orientation of all other water molecules is negligible, as the field is not as large, and only the geometry exerts an effect on orientation. Table 2 gives the average orientation of molecules in the tapered section for the five states of charge. The average defined in the table is taken over all values of number of reservoir molecules, as there is no apparent dependence of orientation on the density in the reservoir. The slope of the plots, for fixed charge, of the cosines vs n_{res} is almost zero, and a linear fit gives correlation coefficients of less than 0.05; in other words, there is effectively no dependence

TABLE 2: Average Cosine for the Five Charge Configurations: Tapered Section

charge configuration	av cos vs *z* axis[a]		av cos vs field of charges[a]	
	dipoles[b]	no dipoles	dipoles[b]	no dipoles
(0,0,0,0)	−0.12 ± 0.10	−0.35 ± 0.15		
(−1,−1,2,2)	0.22 ± 0.10	0.22 ± 0.17	−0.30 ± 0.17	−0.40 ± 0.14
(−2,−2,2,2)	0.45 ± 0.19	0.35 ± 0.14	−0.51 ± 0.19	−0.45 ± 0.12
((−3,1)(3,1)2,2)	0.34 ± 0.18	0.23 ± 0.0.08	−0.62 ± 0.11	−0.63 ± 0.09
(−3,−2,2,3)	0.56 ± 0.15	0.48 ± 0.08	−0.62 ± 0.15	−0.56 ± 0.08

[a] For all cases: cos averaged over all densities, ±standard deviation. [b] Fixed water molecules contribution, rotation allowed to produce net dipole.

of orientation on density. For this reason, only the averages are given for the five charge configurations. Two orientation axes are given: the *z* axis (the vertical axis through the center of the entire volume) and that of the field created by the fixed charges only. This field is not the local field at each molecule, a field which would presumably orient the molecules even more thoroughly, but which is of limited interest with regard to the behavior of the system, as it is not a fixed axis. The orientation with respect to the permanent field created by the fixed charge shows the degree to which the molecules are forced to assume an orientation that will persist. Since the field axis is not always close to the *z* axis, the orientations are not only of opposite sign (which is merely a matter of the direction chosen for the axis) but of different magnitude.

Table 2 suggests there is a maximum orientation that the molecules reach with respect to the *z* axis for any of the charge configurations tested, because of the difference of the orientation of the *z* axis and the field axis. The geometry clearly orients the molecules as well, as can be seen from the zero-charge cases, especially when there is no field from water dipoles.

Table 2 includes both the cases in which the dipoles of the water molecules contributed and those in which they did not. The water dipoles reoriented the water molecules to some extent, so that the orientations are not the same as would be the case if only the fixed molecules provided a permanent field. The other dipoles create a local field which has an orientation that differs from that of the fixed field. The effect is most visible in the zero-charge case, where the orientation is determined by geometric interactions, and the no dipole case is more than two standard deviations from zero (and of opposite sign of that created by all of the permanent charge configurations), while with the dipoles present, the effect is appreciably smaller. The geometry may also, to some extent, orient the molecules away from the field (the average orientation with the *z* axis for the zero-charge case is slightly negative, although only dipole fields exist in this case). The average fields produced by the charge configurations tested are in the range in which the water molecules make the transition from essentially free to sufficiently strongly oriented to be considered tied down by the field. The field of the water dipoles alone is close to the range in which field produces orientation. We note that the orientation with respect to the *z* axis is systematically more positive for the case in which dipoles are present than for the case in which they are not, for four charge configurations (the −1,−1,2,2 case is an exception, but this may be a fluctuation, considering the standard deviation). This is not true for the orientation with respect to the field of the fixed charges, where there is no systematic effect. The field of the dipoles may point the other water molecules in the direction of the *z* axis, an effect overcome by the field of the fixed charges. The fixed charges produce a field larger than the dipoles, but the dipoles are not small enough to neglect.

(3) Density, Cylinder, and Tapered Region. The density of molecules in the cylinder and in the tapered region should show the effects of pressure and electrostriction most directly. We will see that the number of molecules (or density) in both regions increases with the number of molecules in the reservoir, n_{res}, as it must, and is nearly simply proportional; however, the slope of the proportionality does not always keep the ratio of the densities constant, especially in the tapered region.

(a) Cylinder. No Fixed Water Dipoles. We get fairly good straight lines for a plot of density in the cylinder against number of molecules in the reservoir. The slope, if no field effects are present, should be such as to produce a ratio of number of molecules present with $n_{res} = 31$ to number with $n_{res} = 20$ of 31/20 = 1.55. If we combine all five charge cases, we find

$$n_{cyl} = 0.41(\pm 0.068)n_{res} + 2.8(\pm 1.42) \quad (4)$$

The numbers in parentheses are the standard deviations, with the slope and intercept the average of the individual slope and intercept values of the five separate lines (one outlier is largely responsible for the high value of the standard deviation of the intercept). For the individual lines, the correlation coefficients range from 0.76 to 0.96, the average being 0.83. Equation 4 gives a ratio of 1.41 for the number at $n_{res} = 31$ to that at $n_{res} = 20$. It seems safe to regard the cylinder values as proportional to the values in the reservoir, although the slope may be slightly low.

With Water Dipoles. The density in the cylinder can be represented as a function of n_{res} by a straight line. For the four charged configurations, the differences are small, and if the slopes and intercepts are averaged, the resulting line becomes

$$n_{cyl} = 0.26n_{res} + 3.1 \quad (5)$$

where n_{cyl} is the number of molecules in the cylindrical section. The slopes ranged from 0.22 to 0.32, the intercepts from 2.0 to 3.9. For each charge set separately, the correlation coefficients were 0.575−0.764. The ratio of the density at $n_{res} = 31$ to that at $n_{res} = 20$ for eq 4 is 1.34, less than the 1.55 for the reservoir or the 1.41 when no water dipoles are fixed to the walls. It seems that the charge has some effect in the cylinder, and the density increases somewhat less rapidly than would occur in bulk. The electric field makes the ratio of low density to high density somewhat higher than the reservoir ratio. Combined with the slightly greater ratio, and greater slope, obtained in the absence of the water dipoles, it does suggest that the field is sufficient to pull in molecules at low densities, but has more difficulty in doing so at high density, as would be expected (below, we point out that the highest density corresponds to a pressure far greater than that provided by the field, but that the field does correspond to a pressure well above atmospheric pressure).

The uncharged case is a little different. For this case, the slope becomes 0.37, the intercept 1.16, and the correlation coefficient 0.871, indicating a better linear relation. Here, the ratio of the number of molecules in the section when $n_{res} = 31$ to that when $n_{res} = 20$ is 1.48, closer to the 1.55 ratio in the reservoir. It does suggest that the uncharged case is better able to respond to the change in reservoir density than the cases with an appreciable field, consistent with the interpretation in terms of the field producing a change in density especially when the density is low.

(b) Tapered Section. No Water Dipoles. In the tapered section, unlike the cylinder, several cases show what appear to be very large peaks, in a plot of number of molecules in the tapered section as a function of the density in the reservoir. This makes it difficult, however, to carry through the same analysis as with the cylinder section. If plots of the same type as used in analyzing the cylinder are used (number in tapered section vs n_{res}), only one correlation coefficient exceeds 0.7, and three are below 0.4. There is a clear increase in number with increase in n_{res}, but the "peaks" indicate a simple proportionality lacks validity. The magnitude of the peaks, especially for the zero-charge and the (−1,−1,2,2) low-charge cases, is too great to be normal statistical scatter (they exceed 30% changes for changes of 1 in n_{res}). Combined with the different orientational behavior of these two charge cases (Table 2), it suggests that geometric factors can be important in determining how water molecules in the confines of the tapered

region are arranged. It is not clear from the snapshots whether the molecules can sometimes virtually crystallize, but it does seem probable that a form of alignment may occur. (However, the number of molecules is smaller, so the statistics are less powerful in the tapered section; with approximately half the number of molecules, one expects standard deviations approximately 1.5 times as great.)

With Water Dipoles. The results for this region are somewhat different. One can plot the data in the same manner as density vs n_{res}; three fairly good straight lines result: for the charge configuration (−1,−1,2,2), for (−3,1),(−3,1),2,2, and for −3,−2,2,3. These have slopes of 0.27, 0.22, and 0.21, respectively, and correlation coefficients of 0.77, 0.60, and 0.53. For these three cases, the ratio of highest density to lowest is 1.45 (average), fairly close to the 1.55 of the reservoir. The configuration −2,−2,2,2 has a slope that is much smaller, but a correlation coefficient small enough that the scatter dominates the line. Possibly, for this case, the combination of charge position and wall geometry can be stronger than the influence of the external pressure. It cannot be ruled out that there is unusual statistical scatter for a couple of points, however.

The most surprising case is that of zero charge. The average number of molecules in the tapered region is not appreciably different, on average, from that of the other cases, but the slope is only 0.11, with a correlation coefficient of 0.142. Arguments similar to those made for the results with no water dipoles for zero charge suggest, but do not prove, that there must be particular configurations that dominate the distribution of molecules. Note that the orientation with respect to the *z* axis is also of opposite sign of those with charges, but not as large, as the water dipoles may be aligning the molecules to some extent.

(4) Molecular Distribution Functions. Two types of distribution functions can be defined: (i) a radial distribution function, among the water molecules; we will ignore the fixed molecules along the walls, giving a distribution function limited to mobile water molecules; (ii) a distribution with respect to the wall. There is no point in including wall molecules in the latter either, as the program forces them to fixed positions and would thus produce a sharp and uninteresting set of peaks in the distribution. The first distribution function is likely to be rather different from the distribution that one would see in bulk simply because of the presence of the walls, which in most of the volume not only prevents longer distances from appearing but limits the distribution on one side for most of the molecules, so that certain distances cannot appear in the distribution. When no fixed water dipoles are present, the results are averaged from "snapshots" of the configurations at 4000, 5000, and 6000 moves per molecule; when the fixed water dipoles were present, only the values at 6000 moves per molecule were recorded.

(a) Radial Distribution Function. Cylinder. The minimum distance of 2.5 Å between molecules was set in the simulation, and the maximum of approximately 10 Å is determined by the size of the cylinder.

No Fixed Water Dipoles. One can look at the average intermolecular distance of the water molecules, as a function of density in the reservoir, for the same three times. It is again useful to compare a high- and a low-charge case, for several density values. We choose, as before, the minimum density in the reservoir, the normal density, and the high density.

One can also ask the average distance between molecules, as a function of the number of molecules in the reservoir. We calculated this, averaged over the three times (and, as always, three runs for each configuration), as a function of the number of molecules in the reservoir. One should expect, with the cylinder of constant volume and the number of molecules in the cylinder increasing, a decreasing average intermolecular distance. Paradoxically, a weak relation in the other direction was found. The different charge configurations were not distinguishable within statistical error, and the increase in intermolecular distance, on average, was approximately 0.02 Å/molecule in the reservoir. Overall, therefore, the volume occupied per molecule increased about 10% as the number of molecules increased about 40%. We will also understand this better after the distance from the wall has been discussed.

There is one peak in the distribution at approximately 2.9 Å and another near 6.0 Å. At low charge and low density these are not well resolved, and the 6.0 Å peak is small.

In Figure 2 we show the radial distribution functions for three densities and two charge configurations, one zero charge, the other a high-charge case. In Figure 3, the corresponding distributions are shown at normal density for two other charge configurations, one low but not zero, the other high. The net conclusion is that the charge is less important in the cylinder than the density. Further examination of the difference between the cylinder and the tapered section suggests that geometry is also important, as will be suggested by the results discussed under the tapered section.

With Water Dipoles. These snapshots were recorded only at 6000 moves/molecule, so that we cannot test the stability of the peaks. The effects of charge were more easily discernible in these results.

There is one very obvious difference between the two classes of distribution functions: In one, there is a single peak at approximately 2.9 Å, followed by a trailing distribution out to nearly 10 Å, where it disappears. This is characteristic of the uncharged cases from $n_{res} = 20-23$ (and almost the same pattern at 25), as well as the low-charge case (−1,−1,2,2), also up to $n_{res} = 23$. The (−2,−2,2,2) configuration at $n_{res} = 20$ also has the low-charge pattern. With the water dipoles, the charge configurations behave differently, while without the water dipoles they could only be distinguished with difficulty. It is again clear from these results that the water dipoles are nearly as important as the fixed charges, at least for the cylinder, in which the greater proximity of the dipoles is significant.

The second pattern is found in all the other cases, including the high-charge cases, as well as the zero-charge case from $n_{res} = 26-31$. It contains a sharp drop after the first peak, followed by a second peak at approximately 6 Å. Examples are shown in Figure 4. The distribution is somewhat smoother than in the no water dipole cases. However, comparison with the corresponding distributions with no water dipoles shows that the overall location of the peaks in Figure 4b is very close to the locations of the corresponding peaks in that case.

(b) Radial Distribution Function. Tapered Section. The second peak (6.0 Å) present in the cylinder section does not fit into the tapered section, for which the dimensions are smaller. We will consider only the no fixed water dipole case.

No Fixed Water Dipoles. There is a weak relation between the number of reservoir molecules and the average intermolecular distance. For three cases, (−1,−1,2,2), (−2,−2,2,2), and ((−3,1),(−3,1),2,2), the relation with n_{res} is clear, but weak, while for the other two cases, it is almost nonexistent. Paradoxically, as with the cylinder, the larger the number of molecules, again the larger the intermolecular distances. The increase is approximately 0.03 Å × n_{res}, from 20 to 31 molecules in the reservoir, for the three cases in which the relation is "strong". Even for those with a very weak relation, what difference there is is in the same direction.

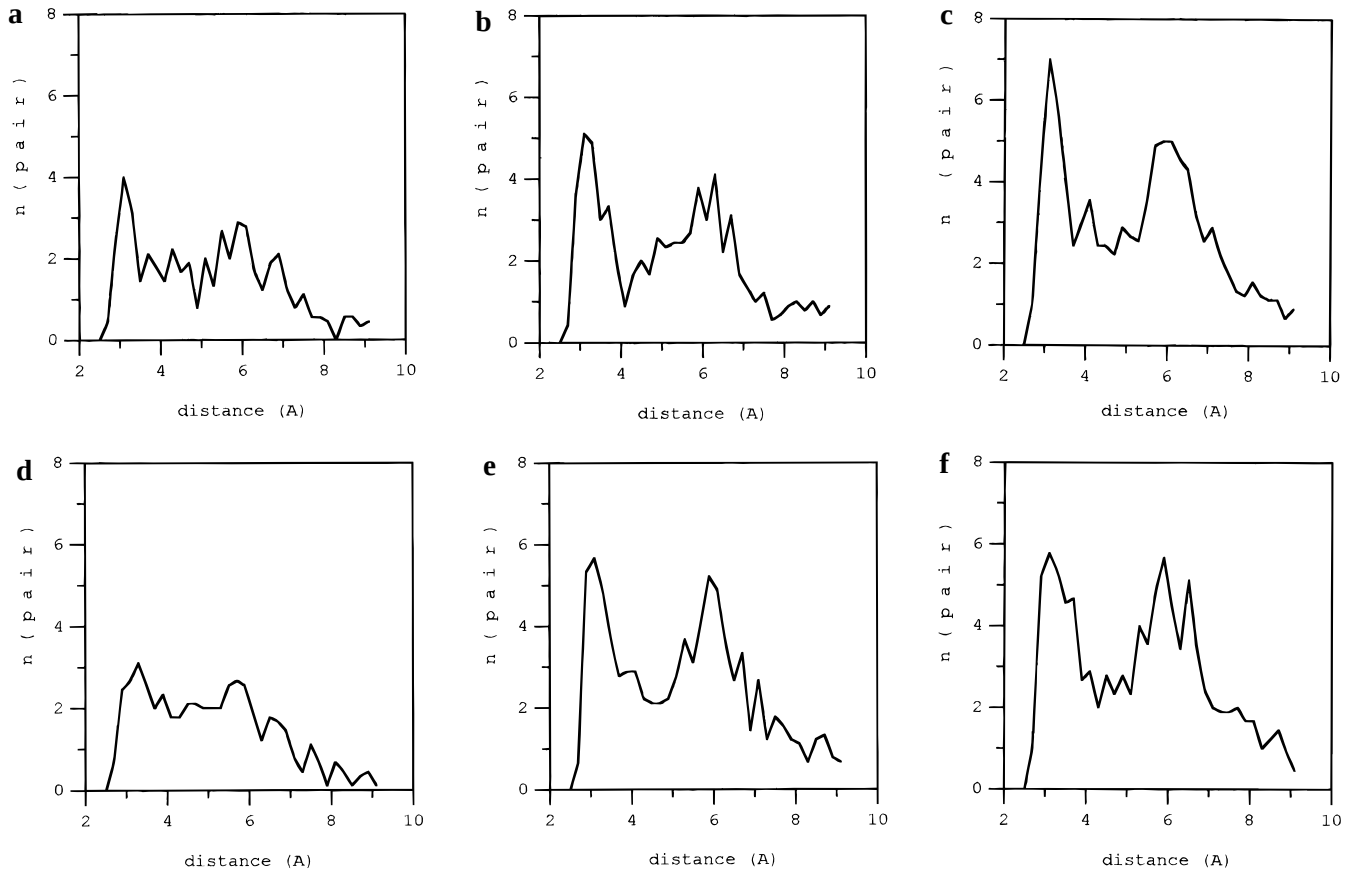

Figure 2. Radial (intermolecular) distribution function in the cylinder, for the case of the no fixed water dipoles; average over snapshots at 4000, 5000, and 6000 moves per molecule, for three runs at each density. Charge configuration (0,0,0,0): (a) $n_{res} = 20$, (b) $n_{res} = 26$, (c) $n_{res} = 31$. Charge configuration ((−3,1),(−3,1),2,2): (d) $n_{res} = 20$, (e) $n_{res} = 26$, (f) $n_{res} = 31$.

(c) Wall Distribution. The effects of charge and pressure here are expected to be complex. Increasing the number of molecules is expected to have two effects, considered from the point of view of the average distance from the wall: first, as the number of molecules increases, the center of the section must fill, placing more molecules at a distance from the wall, and thus increasing the average distance of molecules from the wall. Second, there is the possibility of additional structure, such that the molecules are arrayed in layers along the wall which become more stable as the number of molecules passes a critical value (this phenomenon may behave analogously to a phase transition). This would lead to decreased average distance to the wall.

The charge would be expected to pull the molecules closer to the wall, at least in the tapered section, since water is dipolar, producing electrostriction along the direction normal to the wall. There is, in fact, a general trend in the direction that, at low density, high field may replace some of the higher pressure which corresponds to the higher density. The effect as usual is larger in the tapered section than in the cylinder.

We can use the average distance of the molecules from the wall, a quantity defined by

$$\langle r_w \rangle = \sum_i m_i r_i / \sum r_i \qquad (6)$$

where m_i is the number of molecules in a shell at distance r_i to $r_i + \delta r$ from the wall; we used 0.2 Å for δr.

(i) Cylinder. No Fixed Water Dipoles. We must seek in this distribution the resolution of the paradox of increasing intermolecular distance with increasing density. In fact we find a strong decrease in the average distance of the molecules from the wall in the cylindrical section as the density increases.

$$\langle r_w \rangle = -0.037(\pm 0.004) n_{res} + 3.51(\pm 0.11) \qquad (7)$$

for four of the five charge configurations (the (−3,−2,−2,3) configuration had a slope of only −0.018; the reason for this discrepancy is not obvious). For the lines whose slopes are averaged the correlation coefficients were 0.781 ± 0.131. With the average distance of the molecules to the wall dropping approximately 0.5 Å as the number in the reservoir increases from 20 to 31, there is enough space to include more molecules and still increase the average intermolecular distance as observed. Pulling the molecules toward the wall has the effect of increasing the volume of the cylinder. Increasing pressure, caused by increasing density, at most slightly abetted by increasing field, has the effect of squeezing the molecules slightly further apart. As more molecules approach the wall, the peak location in effect is found on a cylinder that has a larger radius, so that the molecules become further apart.

Both in the cylinder and the tapered section, the wall distribution was saved at three times, at 4000, 5000, and 6000 steps/molecule. The peaks in the distribution change less for the high-charge case. The most stable are those at low and normal density. At zero charge, the peaks are much more mobile and suggest that the molecules move about considerably more. This is a further indication (along with the orientation) that high charge tends to limit the motion of the water, at least within a few angstroms of the wall. At the highest density the space is fairly well filled with water, and the peaks which are so evident at low and moderate density are difficult to see. The much more mobile peaks in the zero-charge case suggest an absence of favored configurations. In the cylinder, in which the fields are in any case smaller than in the tapered section, the peaks are not part of a stable structure when there is zero

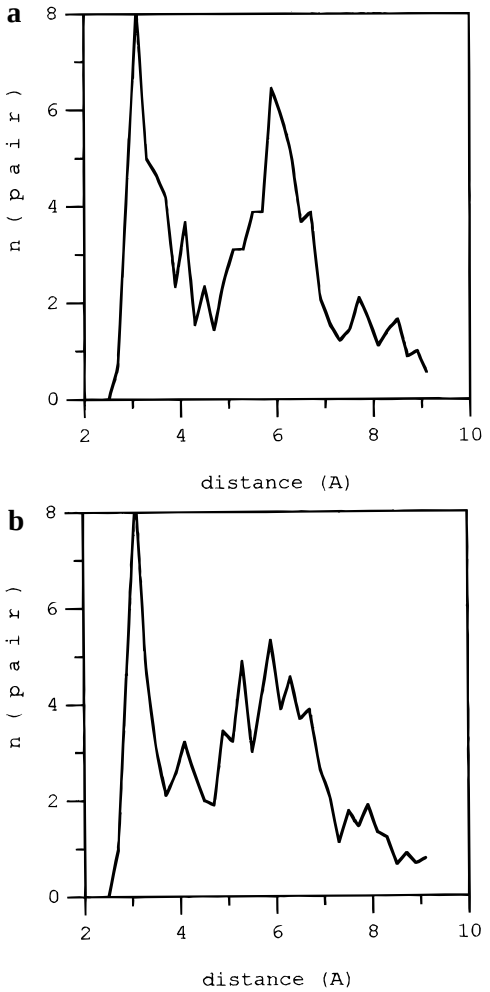

Figure 3. Radial distribution function in the cylinder, again no fixed water dipoles, at normal density only (n_{res} = 26): (a) charge configuration (−1,−1,2,2); (b) charge configuration (−2,−2,2,2). Figures 2 and 3 illustrate the central role played by geometry and density, rather than charge, in the cylinder. At low density the second peak is almost lost, the first weak, regardless of charge. This changes considerably as the density increases.

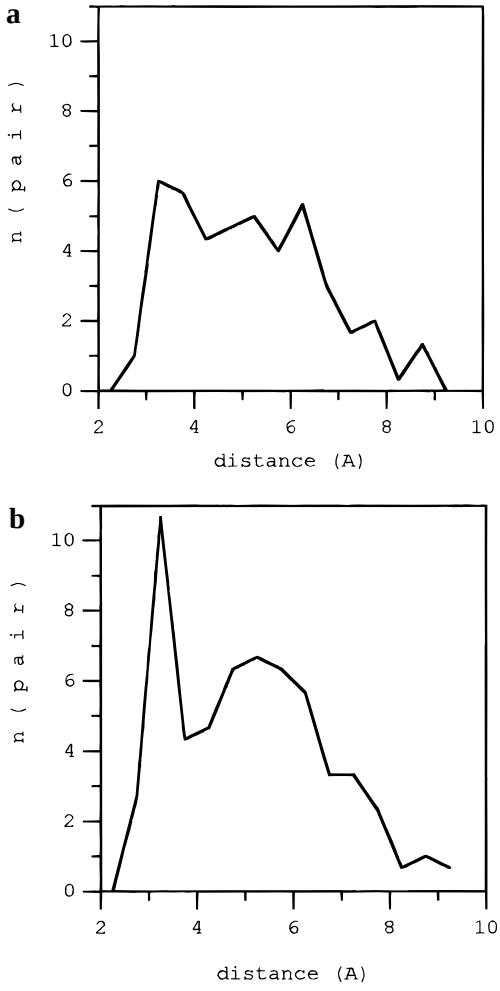

Figure 4. Radial distribution function for the cylinder, with fixed dipoles for the water molecules. Figure is based on 6000 moves per molecule only. (a) Charge configuration (−1,−1,2,2): n_{res} = 22. (b) Charge configuration (−2,−2,2,2): n_{res} = 26. Observe the difference in pattern between a and b, specifically the second peak in b.

charge, and the peak is also somewhat unstable for the (−1,−1,2,2) configuration.

Fixed Water Dipoles. The uncharged case showed two peaks in the number of molecules at a given distance from the wall, as a function of the distance from the wall, at approximately 2.5 and 3.7 Å, for practically all values of n_{res}. In three cases, the magnitude of one or the other peak shrank, but as there did not appear to be any systematic dependence of this on n_{res}, we attribute it to a statistical fluctuation (however, see the discussion of the tapered section, immediately below, in which such peaks appear more regular).

The (−3,−2,2,3) high-charge case appeared to have one more peak, with sharper valleys between peaks. With the fixed water dipoles present, the distance from the wall showed a density dependence similar to that for the case of no fixed water dipoles. The slope, however, was approximately −0.015 Å per reservoir molecule. Possibly the dipoles pulled the molecules closer even at low densities, reducing the slope.

(d) Wall Distribution: Tapered Section. No Fixed Water Dipoles. There are two peaks that appear in these distributions, which were determined separately at 4000, 5000, and 6000 moves/molecule, making it possible to compare the stability of the distributions in time. We find that the distributions with charge are rather stable, while the distributions with no charge are less so. This is shown in Table 3, in which the ratio of the number of molecules in the first peak, total, to those found between peaks, is given, and in Figure 5, in which two examples, one each of high- and zero-charge distributions, are shown separately for 4000, 5000, and 6000 moves/molecule. If the peaks were completely stable—frozen—no molecules would move between the peaks. Further, the three different times would appear identical. The molecules are not that frozen, but there is a considerable difference between the behavior of the molecules in the high- and zero-charge cases.

There is a clear difference between the zero charge case and all others. The (−3,−2,2,3) case has a very large ratio except when n_{res} = 22 or 26; if those two were excluded, the first entry in that column would be 33.7, and the second 21.0. Table 3

TABLE 3: Ratio of First Peak to Interpeak Molecules, Sum over Three Times

range of n_{res}[a]	(0,0,0,0)	(−1,−1,2,2)	(−2,−2,2,2)	((−3,1)(−3,1),2,2)	(−3,−2,2,3)
20−23	6.2	17.1	12.7	16.0	10.6
24−27	7.5	10.8	15.2	11.3	9.6
28−31	7.6	13.9	12.5	48.5	33.0

[a] All four densities in each range were summed and averaged.

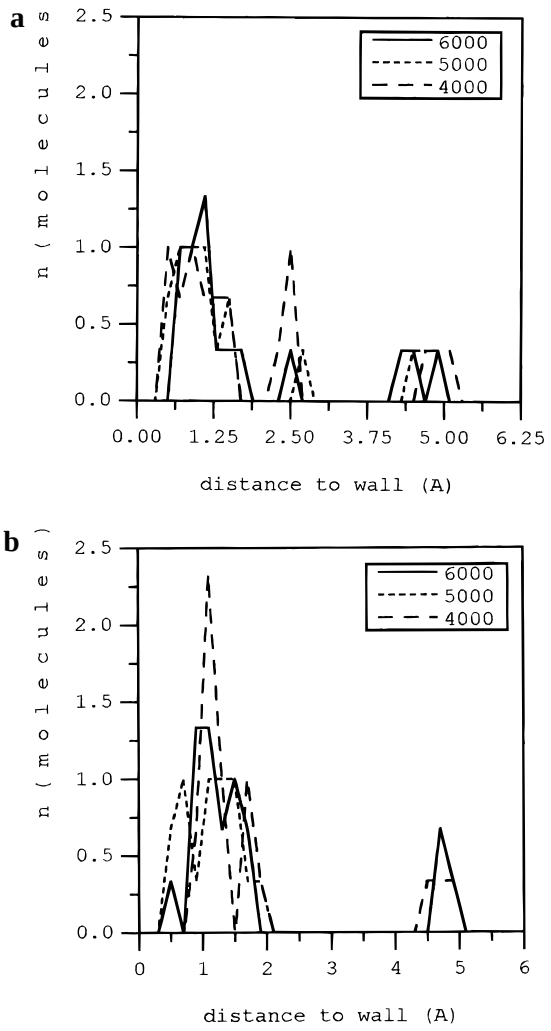

Figure 5. Wall (molecule−wall distance) distribution function, no fixed dipoles. Averages are again from 4000, 5000, and 6000 moves per molecule, this time shown separately to illustrate the difference between the high-charge nearly frozen distribution of molecules and the more mobile zero-charge case. In both cases shown, $n_{res} = 27$. (a) Charge configuration (0,0,0,0). (b) Charge configuration (−3,−2,2,3). For average behavior over all charge configurations and densities, see Table 3. In the tapered section, the charge produces very significant effects.

probably underestimates the overall effect of charge. Most cases would show the same effect as the distributions shown in Figure 5, in which the three different time distributions contrast strongly for high and low charge. There are a few cases (especially the two (−3,−2,2,3) cases just cited) in which the difference largely disappears. Whether this is a symptom of some specific interaction among charge, density, and geometry or a simple statistical accident will require further investigation. Both the data in Table 3 and the appearance of most of the cases suggest that charge significantly restricts mobility.

(5) Electrical Potential. Finally, we have the electrical potential and field throughout the volume. The potential is created in part by the fixed charges and in part by the water. The potential is shown, with no fixed water dipoles, in Figure 6, for several cases: charge configurations (0,0,0,0), (−1,−1,2,2), and ((−3,1),(−3,1),2,2), with the reservoir containing 20, 26, and 31 molecules. These show a sample of the distributions of the electrical potential (the field corresponding to each potential was necessarily also calculated in order to do the simulation, but only the potential is shown). The most obvious features include the regions of high potential near the fixed charges and the induced potentials of opposite sign. In the highest charge configuration, these regions nearly overlap.

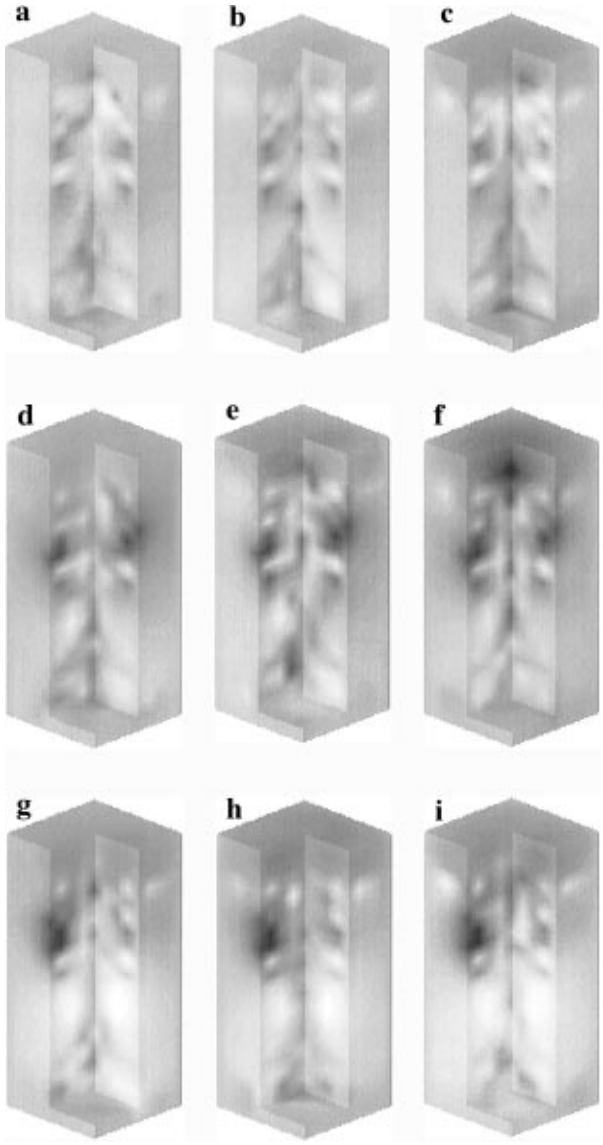

Figure 6. Electrical potential for three charge configurations, with no fixed water dipoles: (a−c) charge configuration (0,0,0,0), with n_{res} = 20, 26, 31, respectively; (d−f) charge configuration (−1,−1,2,2), with n_{res} = 20, 26, 31, respectively; (g−i) charge configuration ((−3,1),(−3,1),2,2), with n_{res} = 20, 26, 31, respectively. The potential is shown as gray scale intensity nominally from −6 V (white) to +6 V (black); see Figure 8 for comparison. The scale is compressed so that it saturates at approximately ±2.5 V, the range within which most of the significant information falls. The entire volume for which the potential is calculated is shown, both that containing water and the boundaries. The "shelf" that appears at the bottom of each figure is 2 Å high, and the distance scale is linear. The major points that are clear from the figures are as follows: (i) The fixed charges dominate the potential. Compare parts g, h, i, with four net negative charges near the tapered region, to d, e, f, with 2 net negative charges, in each case with four positive charges above, and to a, b, c, with no fixed charges at all. In the latter set, the potentials, and consequently the fields, are appreciably less than in the figures with fixed charges. (ii) As can be seen by comparing Figure 8, where each gray scale step is 1.2 V, the fields are extremely large; recall that 1 V/3 A = 3.3×10^9 V m^{-1}. (iii) The effect of density is relatively subtle. There is some softening of the gradient of the potential at the higher densities, this is clearest in the highest charge case (compare g to h to i), especially near the white (negative) areas, which correspond to the tapered region in the model. In parts a, b, and c, with no fixed charge, not only are the potentials clearly smaller, and also their gradients, but the changes with density are larger. The constriction at the bottom of the tapered region shows a more positive potential in b and c.

In the zero-charge case, with only water molecules producing potentials, and these largely averaging, the potentials are smaller,

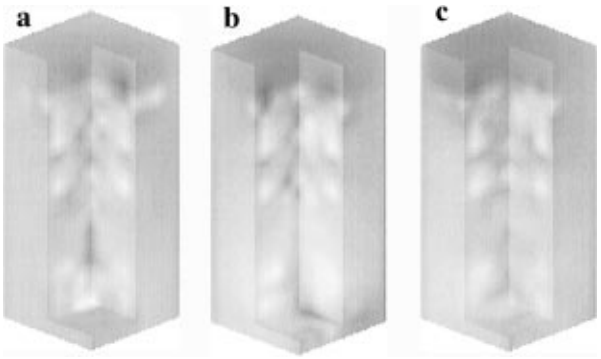

Figure 7. Parts a, b, and c, correspond to parts a, b, and c of Figure 6, for the case in which rotation of water molecules produces fixed dipolar fields at the walls. There are some fixed negative potentials at the top and bottom of the cylinder region which are not found in Figure 6a,b,c. There is more net negative potential in several regions in which there are geometric changes in shape (angles in the boundary). Only the low-density part (a) shows more positive potential at the constriction at the bottom of the tapered region in this case.

Figure 8. Grayscale ruler, for comparison with figures. Each step corresponds to 1.2 V. The scale is compressed at the ends, making the last three steps to white (−6 V) not visible. The top of the scale (black) corresponds to +6 V.

but are still appreciable near the boundaries, especially near the changes in slope of the boundaries. In this case the effect of density is apparent at the highest density (Figure 6c,f), where the high potential is spread over a somewhat wider region than at the lower densities. When fixed charges are present, they dominate the effect of water, at any density. Only in the relatively low charge case of (−1,−1,2,2) charges does the water appear to make a noticeable difference. However, we also show (Figure 7) the zero-charge case with water dipoles; note that the potentials in the tapered region are almost comparable to those in the charged cases, especially the lower charge cases, with no net water dipoles. The water molecules, allowed to rotate, produced more negative potentials in the pore region.

Quantitatively the fields are huge. There is a drop of several hundred millivolts, up to a volt, over short distances, down to 3 Å. This leads to fields in the pores, at maximum, of around 3×10^9 V m^{-1}. The fields in the surrounding dielectric can be even larger.

IV. Discussion and Conclusions

(1) Pressure Compared to Electric Field. Both pressure and electric field produce major effects on the water in a pore, but the geometry modifies these effects to a great degree. The field, although large, is not so large that it can compare to the pressure equivalent to the difference in density in the reservoir. The Tait equation describing the pressure−volume relation of water, although originally derived for the range up to 500 atmospheres (50 MPa),[37] is actually quite good to pressures above 10 GPa,[38] and thus above our maximum pressure. We

TABLE 4: Pressures Corresponding to Increased Numbers of Molecules in the Reservoir

number of reservoir molecules	pressure in reservoir (MPa)
27	93
28	200
29	330
30	480
31	660

can use the Tait equation in the form

$$V/V_0 = 1 - A \ln((B + P)/(B + P_0)) \qquad (8)$$

where V is the volume of the water, V_0 is a reference volume, $A = -0.1368$, and B, at 25 °C, is 3.00×10^3 bar, or 3.00×10^2 MPa.[37] We take the reference state at 1 atm = 0.1 MPa and can therefore neglect the P_0 term. Using this equation and taking the volume to be inversely proportional to the number of molecules in the reservoir, we can get the pressure for those values of pressure above 1 atm (there is apparently no evidence concerning the validity of the equation below this pressure, and it would be surprising if it were valid). This corresponds to 26−31 molecules in the reservoir. The pressures are given in Table 4.

The Tait equation also makes it possible to obtain an estimate of the $\Delta(PV)$ energy for the reservoir, by integrating the equation up to the maximum pressure. When the reservoir contains 31 molecules, the maximum, this energy is approximately 2×10^{-19} J for the reservoir, compared with over 9×10^{-19} J for the reservoir total. The $\Delta(PV)$ energy is not negligible, but not large enough to change the main qualitative conclusions. For smaller numbers of molecules in the reservoir, the $\Delta(PV)$ energy drops faster than the total energy.

Pressure has units of energy density; Pa = J m^{-3}. We can compare the pressures to the energy density for the electric field, given by $W = (1/2)\epsilon E^2$. If $E = 10^9$ V m^{-1}, then one gets 4.4 MPa; if $E = 3 \times 10^9$ V m^{-1}, the pressure corresponds to 40 MPa. Therefore, any electric field effects are unlikely to be consequences of pressure from the electrostriction, but it does suggest that fields of such high magnitude do in fact correspond to fairly high pressure. Furthermore, the fields are large enough to at least partially make up for the reduced pressure produced by reduced numbers of molecules in the reservoir. Ferchmin and Ferchmin-Danielewicz[17] found that fields could compress water to essentially double the normal density value at ordinary pressure, but they were dealing with fields exceeding those we have just used in the calculation by over an order of magnitude, leading to pressures more than 100 times greater. They did find that properties of the water under pressure generated by the field were comparable to those produced by ordinary pressure.

Let us first consider the density in the cylinder with at least 26 molecules in the reservoir. From eq 4, the ratio of number of molecules in the cylinder with 31 in the reservoir is only 1.15 times the number with 26 molecules, slightly less than 31/26 = 1.19. With fixed water dipoles, the ratio is 1.13, for all charged cases. By comparison, with zero charge (even with water dipoles), the ratio in the cylinder is 1.18, very close to 1.19. The field seems to pull more molecules in at low densities than at high, an effect which is perhaps to be expected; an alternate form of the Tait equation is

$$\beta = -A/(B + P) \qquad (9)$$

where β is the compressibility. The compressibility decreases just in the range of the pressures we expect in our results,

reaching approximately half the original value when the number of reservoir molecules reaches 29, and about one-third at 31 (based on Table 4). The effective electrostriction might be expected to be less at the highest pressures. However, as the same dependence of number of cylinder molecules vs reservoir molecules was at least approximately maintained down to much less than the equilibrium number of molecules, this explanation is probably too simple, and we must expect that geometric factors and interaction with the wall also play a role in understanding the results.

The density in the tapered region is irregular as a function of the number of molecules in the reservoir. The geometry, the electrostriction, and the pressure interact to produce configurations that appear to be stable. It appears that attempting to treat the system as though it were a bulk medium could not produce intelligible results.

(2) Orientation. In the tapered region the molecules are strongly oriented by the field and the geometry, as can be seen from Table 2. As the alignment with respect to the *z* axis is non-negligible for zero charge, especially in the absence of fields created by water dipoles, we can be reasonably certain of the importance of wall interactions. The orientation is sufficient to nearly match, in magnitude, that provided by the field. The highest charge densities do produce the strongest alignment, as expected.

(3) Molecular Distributions. The intermolecular distances are affected by the field mainly in the tapered region, as shown by eq 7 and the results discussed in section III.4.b,c. The distances to the wall seem to be determined largely by density and the geometry of the tapered region; however, the considerable difference between the zero-charge results and the nonzero-charge configurations shown in Table 3 and Figure 5, for the mobility, suggests that the actual behavior of the water molecules does depend strongly on the field, especially in the tapered section. For the cylinder, the field is much less important.

Electrostriction is seen most strongly in the wall distributions in the tapered section; molecules in both the cylinder and the tapered region are pulled closer to the wall by high-charge configurations, but more so in the tapered section. This helps to explain the complex behavior of the density. With molecules forced into configurations which are other than those that would be assumed in the absence of the field, the density must also change. Furthermore, the alignment is itself a function of the density. The density distributions provide further evidence for the interaction of electric field and density, and for the interaction of molecules with field and with the wall in the confined geometry. Combined with the orientation data, these results provide evidence for significantly decreased mobility, on average, for the water molecules in the tapered region, in particular, in high-charge configurations. None of this is surprising, but it does help to secure a sense of the magnitude of the fields required and of the necessary geometry.

Several other workers have investigated the distribution of molecules in pores. Lynden-Bell and Rasaiah[39] found a cylindrical solvation shell in a cylindrical pore, with some effects on the next layer. The strongest effects were of course in the narrowest cylinders. Sansom et al.[27] looked also at tapered pores, again seeing solvation shells along the wall. Lee and Rossky,[40] simulating water along a flat surface, found structure mainly in the first layer and essentially no effect beyond 10 Å distance from the surface; for purposes of comparison with our work, in which the diameter of the tapered section is less than 10 Å, this amounts to a major effect.

(4) Energy. To an excellent approximation, the energy of the molecules not in the reservoir depends linearly on the number of molecules. The higher fields are associated with lower energy. The interaction between the electric field and the density does not have a large effect on the energy, and there is no observable minimum in energy at the bulk density. The statistics are just adequate to show weak nonlinearity in the energy−density relation which is consistent in sign among the various charge configurations. The interaction of water with the field in the tapered section is strong and proportional to the number of charges. In this critical section, the interaction with charge (absent interfering dipoles) is nearly as strong as the sum of other energy interactions of the molecules, at the highest charge. There is a noticeable effect even in the cylinder, although, as is to be expected, it is weaker.

(5) Electrical Potential. In the pore, especially the tapered section, the charges strongly influence the water. The orientation of the water in the pore follows the field produced by the charges. Moving the charges, or removing them, possibly by having them neutralize each other, is sufficient to drastically change the behavior of the water, as is most clear from the energy and orientation. Although in this work we did not include an ion in the pore, probably the behavior would be similarly affected. (We did see such effects in earlier work, with a truncated pore, and only the standard density.[35])

(6) Conclusions. The behavior of water in a pore is affected by the electric fields in the pore, as well as the wall. In addition, if the density is varied by altering the effective pressure with which the pore is in equilibrium, the effects of the field and the wall are modified. The orientation, the density, the distribution of the molecules with respect to the wall and to each other all suggest that the water molecules are made more rigid and are arranged differently than in bulk when in the pore, especially in the narrowest section of the pore. Based on our results, there is no clear evidence for the existence of a phase transition. The water may be more nearly glassy; however, the results on dynamics in some references cited above[16,27,39,40] suggest that the lifetime of the water would probably not exceed a nanosecond in any given position, *unless somehow effectively bound to the wall*. Previous studies with water which moved slowly, especially by Ferchmin and Ferchmin-Danielewicz,[17] were those at the highest field, as would be expected. The mobile water, even in the tapered section, under the conditions considered here probably does not reach macroscopically slow motions. As we did not study the dynamics, we cannot add to this discussion. On the other hand, it is known that water remains in position in the interior of proteins long enough to appear as fixed in X-ray structures,[24,27,42] so that it is not implausible that at least boundary water is in fact placed for a time long compared to gating in a given location (the X-ray data do not extend to orientation). We had not expected the water molecules fixed to the wall, when allowed to rotate freely, to produce a net dipole anything like that which we observed.

On the basis of our calculations and these results, it should be possible for the water to be rearranged by movement of charge in the wall, and the movement of charge would be coupled to at least transient increased fluidity of the water in the narrow part of the pore. Small pores generally do slow molecular, polar liquids, as was shown in measurements by Xu et al.[43] Sansom et al.[28] found that the water moved more slowly in the narrower tapered pores, and their calculations showed a gradient of water mobility. They did not, however, apply an electric field. How strong an effect on rates the combination of field, taper, and possibly pressure would be is hard to estimate

from their results, or from ours. Time resolution in small pores in high electric fields remains for further work.

The most obvious result, however, is the difference between the cylinder and the tapered region, as shown by orientation, distribution of the molecules with respect to each other and to the wall, and density in response to external changes in density, electrical potential, and pressure. It is clear that small changes in the local geometry should be able to make significant changes in the behavior of the water in the neighborhood.

The consequence for protein behavior of the difference in behavior of the two regions may be of interest. Whether a single mutation, by changing the local geometry, or, transiently, even the rearrangement of a side chain, can make a significant change in the behavior of water in a pore or a channel should be an important subject for further investigation.

Acknowledgment. This work has been supported in part by an instrumentation grant from NSF and by PSC/CUNY grants to M.E.G.

References and Notes

(1) Timasheff, S. N. *Annu. Rev. Biophys. Biomol. Struct.* **1993**, *22*, 67.
(2) Honig, B.; Sharp, K.; Yang, A.-S.; *J. Phys. Chem.* **1993**, *97*, 1101.
(3) Wei, Y.-Z.; Kumbarkhane, A. C.; Sadeghi, M.; Sage, J. T.; Tian, W. D.; Champion, P. M.; Sridhar, S.; McDonald, M. J. *J. Phys. Chem.* **1994**, *98*, 6644.
(4) Bellisent-Funel, M.-C.; Texeira, J.; Bradley, K. F.; Chen, S. H.; Crespi, H. L. *Physica B* **1992**, *180*−*181*, 740.
(5) Gutmann, M.; Tsfadia, Y.; Masad, A.; Nachiel, E. *Biochem. Biophys. Acta* **1992**, *1109*, 141.
(6) Parsegian, V. A.; Rau, D. C. *J. Cell Biol.* **1984**, *99*, *pt2*, 196s.
(7) Rau, D. C.; Lee, B.; Parsegian, V. A. *Proc. Natl. Acad. Sci. U.S.A.* **1984**, *81*, 2621.
(8) Zimmerberg, J.; Bezanilla, F.; Parsegian, V. A. *Biophys. J.* **1990**, *57*, 1049.
(9) Handa, Y. P.; Zakrzewski, M.; Fairbridge, C. *J. Phys. Chem.* **1992**, *96*, 8594.
(10) van Miltenberg, J. C.; van der Eerden, J. P. *J. Cryst. Growth* **1993**, *128*, 1143.
(11) Epstein, B. R.; Foster, K. R.; Mackay, R. A. *J. Colloid Interface Sci.* **1983**, *95*, 218.
(12) Foster, K. R.; Epstein, B. R.; Mackay, R. A. *J. Colloid Interface Sci.* **1982**, *88*, 23.
(13) Derjaguin, B. V.; Churaev, N. V. *Langmuir* **1987**, *3*, 607.
(14) Green, M. E.; Lewis, J. *Biophys. J.* **1991**, *59*, 419.
(15) Toney, M. F.; Howard, J. N.; Richer, J.; Borges, G. L.; Gordon, J. G.; Melroy, O. R.; Weisler, D. G.; Yee, D.; Sorenson, L. B. *Nature* **1994**, *368*, 444.
(16) Toney, M. F.; Howard, J. N.; Richer, J.; Borges, G. L.; Gordon, J. G.; Melroy, O. R.; Weisler, D. G.; Yee, D.; Sorenson, L. B. *Surf. Sci.* **1995**, *335*, 326.
(17) Danielewicz-Ferchmin, I.; Ferchmin, A. R. *J. Phys. Chem.* **1996**, *100*, 17281.
(18) Outhwaite, C. W.; Bhuiyan, L. B. *J. Chem. Soc., Faraday Trans. 2* **1983**, *79*, 707.
(19) Attard, P.; Mitchell, D. J.; Ninham, B. W. *J. Chem. Phys.* **1988**, *88*, 4987.
(20) Lee, S. H.; Rasaiah, J. C.; Hubbard, J. B. *J. Chem. Phys.* **1987**, *86*, 2383.
(21) Brodsky, A. M.; Watanabe, M.; Reinhardt, W. P. *Electrochim. Acta* **1991**, *36*, 1695.
(22) Watanabe, M.; Brodsky, A. M.; Reinhardt, W. P. *J. Phys. Chem.* **1991**, *95*, 4593.
(23) Lockhart, D. J.; Kim, P. S. *Science* **1992**, *257*, 947.
(24) Lancaster, C. R. D.; Michel, H.; Honig, B.; Gunner, M. R. *Biophys. J.* **1996**, *70*, 2469.
(25) Green, M. E.; Lu, J. *J. Colloid Interface Sci.* **1995**, *171*, 117.
(26) Wiggins, P. *Prog. Polym. Sci.* **1988**, *13*, 1.
(27) Thanki, M.; Thornton, J. M.; Goodfellow, J. *J. Mol. Biol.* **1988**, *202*, 637.
(28) Sansom, M. S. P.; Kerr, I. D.; Breed, J.; Sankararamakrishnan, R. *Biophys. J.* **1996**, *70*, 693.
(29) Sankararamakrishnan, R.; Adcock, C.; Sansom, M. S. P. *Biophys. J.* **1996**, *71*, 1659.
(30) Dorman, V.; Partenskii, M. B.; Jordan, P. C. *Biophys. J.* **1996**, *70*, 121.
(31) Sancho, M.; Partenskii, M. B.; Dorman, V.; Jordan, P. C.; *Biophys. J.* **1995**, *68*, 427.
(32) Hemley, R. J.; Jephcoat, A. P.; Mao, H. K.; Zha, C. S.; Finger, L. W.; Cox, D. E. *Nature (London)* **1987**, *330*, 737.
(33) Polian, A.; Grimsditch, M. *Phys. Rev. B* **1983**, *27*, 6409.
(34) Gilson, M. K.; Rashin, A.; Fine, R.; Honig, B. *J. Mol. Biol.* **1985**, *184*, 503.
(35) Lu, J.; Green, M. E. *Prog. Colloid and Polym. Sci.* **1997**, *103*, 121.
(36) Ahlstrom, P.; Wallqvist, A.; Engstrom, S.; Jonsson, B. *Mol. Phys.* **1989**, *68*, 563.
(37) Gregory, J. K.; Clary, D. C.; Liu, K.; Brown, M. G.; Saykally, R. J. *Science* **1997**, *275*, 814.
(38) Moelwyn-Hughes, E. A. *Physical Chemistry*, 2nd ed.; Macmillan: London, 1961; p 690.
(39) Munro, R. G.; Block, S.; Mauer, F. A.; Piermarini. *J. Appl. Phys.* **1982**, *53*, 6174.
(40) Lynden-Bell, R. M.; Rasaiah, J. C. *J. Chem. Phys.* **1996**, *105*, 9266.
(41) Lee, S. H.; Rossky, P. J. *J. Chem. Phys.* **1994**, *100*, 3334.
(42) Otting, G.; Liepinsh, E.; Wuthrich, K. *Science* **1991**, *254*, 974.
(43) Xu, S.; Zhang, J.; Jonas, J. *J. Chem. Phys.* **1992**, *97*, 4564.